

1 Article

2 **Macrocyclic tetramers – structural investigation of**
3 **peptide-peptoid hybrids**4 Claudine Nicole Herlan ¹, Anna Sonnefeld ², Thomas Gloge ², Julian Brückel ¹, Luisa Chiara
5 Schlee ¹, Claudia Muhle-Goll ², Martin Nieger ³ and Stefan Bräse ^{1,4*}6 ¹ Institute of Organic Chemistry, Karlsruhe Institute of Technology, Fritz-Haber-Weg 6, 76131 Karlsruhe,
7 Germany8 ² Institute for Biological Interfaces 4, Karlsruhe Institute of Technology, Hermann-von-Helmholtz-Platz 1,
9 76344 Eggenstein-Leopoldshafen, Germany10 ³ Department of Chemistry, University of Helsinki, P.O. Box 55 (A.I. Virtasen aukio 1), FIN-00014 University
11 of Helsinki, Finland.12 ⁴ Institute of Biological and Chemical Systems—Functional Molecular Systems, Karlsruhe Institute of
13 Technology, Hermann-von-Helmholtz-Platz 1, 76344 Eggenstein-Leopoldshafen, Germany.

14 * Correspondence: stefan.braese@kit.edu

15 Received: date; Accepted: date; Published: date

16 **Abstract:** Outstanding affinity and specificity are the main characteristics of peptides, rendering
17 them interesting compounds for basic and medicinal research. However, their biological
18 applicability is limited due to fast proteolytic degradation. The use of mimetic peptoids overcomes
19 this disadvantage, though they lack stereochemical information at the α -carbon. Hybrids composed
20 of amino acids and peptoid monomers combine the unique properties of both parent classes.
21 Rigidification of the backbone increases the affinity towards various targets. However, only little is
22 known about the spatial structure of such constrained hybrids.

23 The determination of the three-dimensional structure is a key step for the identification of new
24 targets as well as the rational design of bioactive compounds. Herein, we report the synthesis and
25 the structural elucidation of novel tetrameric macrocycles. Measurements were taken in solid and
26 solution states with the help of X-ray scattering and NMR spectroscopy. The investigations made
27 will help to find diverse applications for this new, promising compound class.

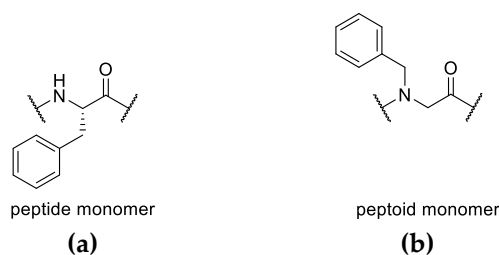
28 **Keywords:** peptidomimetics; tetramers; macrocycles; spatial structure.

29

30 **1. Introduction**

31 Peptides, a structurally and functionally diverse class of macromolecules, are involved in all
32 parts of life. Their unique properties render them highly promising compounds for biochemical and
33 medicinal research [1, 2]. However, peptides come along with some drawbacks limiting their
34 applicability as selective therapeutics: fast proteolytic degradation resulting in low bioavailability
35 and improvable physicochemical properties [3, 4].

36 Cyclization has been shown to increase proteolytic resistance and even the binding affinity and
37 specificity of linear peptides [5, 6]. Spatially fixed arrangements of functional moieties arouse
38 outstanding bioactivities, especially in small cyclic peptides [7-12]. Another approach to improve the
39 bioavailability of linear peptides while maintaining their unique characteristics has been modifying
40 the individual building blocks [13, 14]. The formal shift of the side chain from the α -carbon to the
41 nitrogen atom results in peptoids, which mimic the structure of their parent compounds but lack
42 pivotal motifs affecting the spatial arrangement (Figure 1) [15-18].



43 **Figure 1.** L-Phenylalanine is an example of an amino acid as the monomer of a peptide (a) and its
 44 respective peptoid monomer (b).

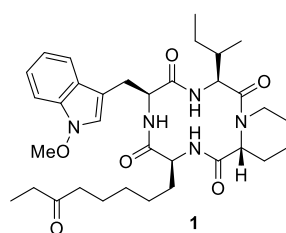
45 N-alkylation in peptoids prevents the formation of backbone hydrogen bonds which are crucial
 46 for stabilizing secondary structures in related peptides. The absence of the hydrogen bond donor
 47 results in enhanced conformational flexibility that comes along with increased *cis/trans*-amide
 48 isomerism [19-21]. To constrain their conformational flexibility, peptoids of different sizes have been
 49 cyclized [22-29]. Structural studies of these macrocycles revealed defined geometries entailing
 50 distinct *cis-trans* sequences depending on the size and the type of side chains [19, 20, 22].

51 Besides peptoid macrocycles, several studies on cyclic, N-methylated peptides have been
 52 reported [30-35]. However, little is known about the spatial structure of macrocycles that are built up
 53 of natural amino acids and peptoid monomers. These hybrid structures combine the unique
 54 selectivity and affinity of peptides with the outstanding metabolic stability of peptoids. To date, only
 55 a few representatives of this compound class, which holds great promise for future biochemical and
 56 medical research, are known [36-41]. Understanding the spatial structure of the peptide-peptoid
 57 hybrids allows for the search for potential targets and enables rational drug design.

58 Herein, we report the synthesis and structural elucidation of tetramers with different ratios of
 59 amino acids to peptoid monomers. To constrain their conformational flexibility, macrocycles made
 60 up of four monomers were built by head-to-tail cyclization. Crystallographic data and NMR studies
 61 were used to determine the three-dimensional (3D) structures of the resulting peptide-peptoid
 62 hybrids in solid and solution states. This structural investigation can be a stepping stone for further
 63 research on this promising compound class.

64 2. Results and Discussion

65 Initially, we aimed to synthesize a congener library of the cyclic tetrapeptide apicidin (1, Figure
 66 2) [42]. The natural fungal metabolite is known for its ability to inhibit histone deacetylases (HDAC)
 67 and thus to modify the gene expression in eukaryotic cells [43-46].



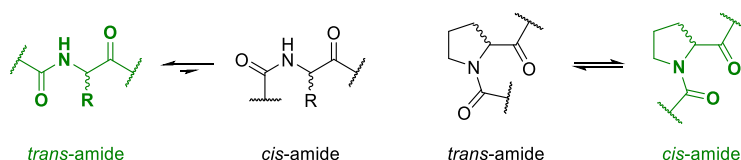
68 **Figure 2.** The cyclic tetrapeptide apicidin (1).

69 Our aim was the design of apicidin derivatives capable of the inhibition of the Wnt/ β -catenin
 70 signaling pathway. Thus, our structures lacked the characteristic L-2-amino-8-oxodecanoic acid
 71 (Aoda), which is critical for the HDAC activity of apicidin (1) [46]. While analyzing the novel
 72 structures, we have observed that replacing individual amino acids with peptoid monomers has an
 73 interesting influence on the spatial structure of the macrocycles. Herein, we report our findings based
 74 on selecting apicidin congeners with different peptide to peptoid ratios.

75 Although various chemically and structurally diverse side chains were incorporated into the
 76 library of apicidin derivatives, all congeners had an aromatic amino acid and the cyclic, N-alkylated

77 amino acid proline in common. Proline was chosen due to its similarity to the building block of the
 78 lead structure apicidin (1), namely pipercolic acid, and its decreased energy barrier for *cis-trans*-
 79 isomerism [47-49].

80 Peptide bonds are constrained in their free rotatability due to their strong π -character. The
 81 energy distribution favors two distinct dihedral angles representing *cis*- and *trans*-amide bonds
 82 (Scheme 1) [50, 51].

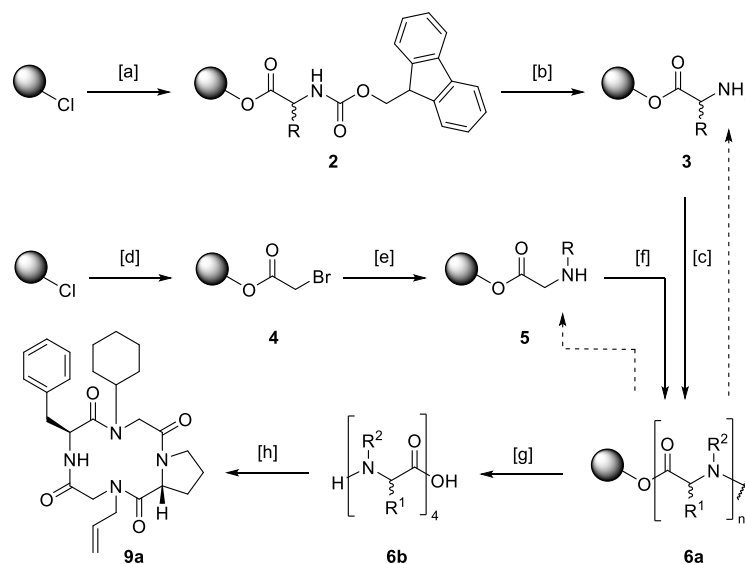


83 **Scheme 1.** The *cis-trans*-isomerism of peptide bonds.

84 Due to the steric hindrance of their side chains, most amino acids form *trans*-conformations with
 85 high energy barriers for *cis-trans*-isomerism [50, 51]. The unusual structure of proline results in an
 86 equimolar distribution of both the *cis*- and the *trans*-conformation when incorporated into a
 87 polypeptide [47-49]. In nature, isomers of proline are known as loop inducers due to *cis*-bond
 88 formation [52, 53]. As it is assumed that backbone *cis*-conformations can facilitate the ring closure of
 89 tense cyclic tetramers [8, 54, 55], proline was the building block of choice for the design of different
 90 macrocycles.

91 2.1. Synthesis of macrocyclic tetramers

92 Hybrid structures consisting of amino acids and peptoid monomers were built upon solid
 93 support. The synthetic protocol involved the well-known solid-phase peptide synthesis described by
 94 Merrifield [56] as well as the submonomer method for the assembly of peptoids published by
 95 Zuckermann [57] (Scheme 2).



96 **Scheme 2.** Synthetic protocol of cyclic tetramers. [a]: Fmoc-protected amino acid, *N,N'*-
 97 diisopropylethylamine (DIPEA), *N*-methyl-2-pyrrolidone (NMP), 21 °C, 16 h; [b]: piperidine,
 98 dimethylformamide (DMF), 21 °C, 3 × 5 min; [c]: Fmoc-protected amino acid, *N,N'*-
 99 diisopropylcarbodiimide (DIC), hydroxybenzotriazole, NMP, 21 °C, 4 h; [d]: bromoacetic acid,
 100 DIPEA, DMF, 21 °C, 1 h; [e]: amine, DMF, 21 °C, 1-16 h; [f]: 1. bromoacetic acid, DIC, DMF, 21 °C,
 101 30 min; 2. amine, DMF, 21 °C, 1-16 h; [g]: hexafluoroisopropanol, methylene chloride, 21 °C, 16 h; [h]:
 102 HATU, DIPEA, DMF, 21 °C, 30 h.

103 The attachment of the C-terminal amino acid (\rightarrow 2) or bromoacetic acid as the first submonomer
 104 of a peptoid building block (\rightarrow 4) to a 2-chlorotriyl chloride polystyrene resin was performed under
 105 basic conditions. In the case of amino acids, the Fmoc-protection group was cleaved using a mixture
 106 of 20% piperidine in DMF, resulting in the free primary amine 3. To build up peptoids, bromoacetic
 107 acid was substituted by any desired amine (\rightarrow 5). Depending on the sequence, free amines were either
 108 coupled to an amino acid or bromoacetic acid. Diisopropylcarbodiimide was used as a coupling agent
 109 in both cases. To avoid racemization, hydroxybenzotriazole was added for the attachment of amino
 110 acids.

111 Acetylation and substitution and amino acid coupling and deprotection were carried out until
 112 the desired linear precursor 6 was constructed. Cleavage was performed under mildly acidic
 113 conditions releasing a linear tetramer capable of a head-to-tail cyclization. The ring closure was
 114 carried out following a protocol by Aldrich [58] with the help of the potent coupling reagent
 115 [Dimethylamino(triazolo[4,5-b]pyridin-3-yloxy)methylidene]-di-methylazanium hexafluoro-
 116 phosphate (HATU). This iminium salt is known for its potency in energetically unfavorable
 117 couplings, cyclizing constrained tetrapeptides [8, 59, 60]. To avoid favored side reactions like
 118 cyclodimerizations [55, 61, 62], a 5.00 mM solution of the respective linear precursor was added
 119 dropwise to a 2.40 mM solution of HATU.

120 Reactive moieties of side chains were masked with protecting groups. Deprotection was
 121 performed immediately after the cyclization step. After ten or eleven reaction steps, respectively,
 122 the synthetic protocol yielded cyclic tetramers, which required only a single purification step at the end
 123 of the reaction sequence. Purification was carried out *via* preparative reversed-phase HPLC, and
 124 product formation was confirmed *via* MALDI-TOF mass spectrometry.

125 In an initial library, several macrocyclic tetrapeptides of general structure 7 were synthesized.
 126 To match the model structure apicidin (1), proline was incorporated in its D-configuration. The
 127 remaining amino acids were applied in their L-configuration. To avoid diketopiperazine formation
 128 [63, 64], D-proline was incorporated as the third building block during the modular solid-phase
 129 synthesis. Approaches with proline as N-terminal building block yielded low amounts of the desired
 130 macrocycles (data not shown). It was assumed that the low nucleophilicity of the secondary amine
 131 prevented cyclization.

132 For this reason, the sequence of the linear precursors was changed in such a way that a primary
 133 amine was in the N-terminal position (R¹). Cyclization of these precursors then led to moderate yields
 134 of the corresponding macrocycles. Nine derivatives with structural similarity were selected to
 135 represent the library of macrocyclic tetramers (Table 1).

136 **Table 1.** Cyclic tetrapeptides of general structure 7 and their respective yields over ten or eleven
 137 reaction steps.

7

Macrocycle	R ¹	R ²	R ³	Yield
7a				22%
7b				46% ^[1]
7c				57%
7d				44%
7e				56%

7f				36%
7g				22% ^[1]
7h				38%
7i				54%

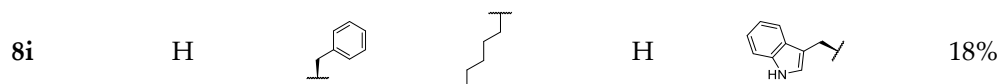
138 ^[1] Yield over eleven reaction steps.

139 The *N*-terminus of the linear precursors (position R¹) consisted of branched aliphatic or aromatic
 140 amino acids. In position R², different alkyl side chains were incorporated. The *C*-terminus (position
 141 R³) was built by either L-phenylalanine or L-tryptophan. Ring closure was carried out by amidation
 142 of the *N*-terminal amine (R¹) with the carboxyl function of the *C*-terminal, aromatic amino acid (R³).
 143 The use of different building blocks did not influence the overall yield of the reaction. Even additional
 144 deprotection steps (compounds **7b** and **7g**) had no clear effect on the yields of the macrocyclic
 145 tetrapeptides. On average, the cyclic tetramers were isolated in 42% ± 13 overall yield.

146 In a second library, individual amino acids were replaced by a peptoid monomer. Peptoids are
 147 peptidomimetics that promise high metabolic stability and outstanding biological activity [15-17].
 148 Compared to peptides, the side chain is formally shifted from the α -carbon to the backbone nitrogen
 149 atom. This comes with high conformational flexibility as the amide nitrogen loses its capability to
 150 serve as a hydrogen bond donor. Moreover, the modification of the amide nitrogen lowers the energy
 151 barrier of *cis/trans* isomerization [18, 19, 65, 66]. However, a beneficial effect of this enhanced
 152 flexibility on the cyclization reaction was not observed. The nine macrocyclic hybrids representing a
 153 library composed of tetramers with three amino acids and one peptoid monomer were isolated in
 154 31% ± 14 overall yields (Table 2).

155 **Table 2.** Cyclic tetramers of general structure **8** and their respective yields over ten reaction steps.

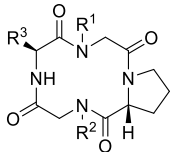
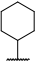
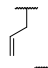
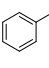
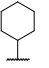
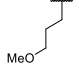
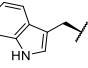
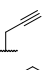
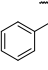
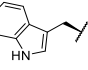
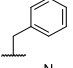
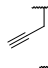
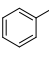
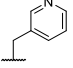
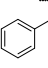
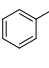
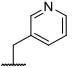
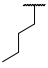
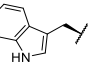


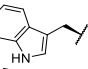
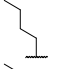
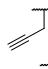
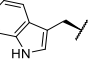

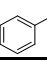
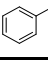
Macrocycle	R ¹	R ²	R ³	R ⁴	R ⁵	Yield
8a		H	H			28%
8b		H	H			8.4%
8c		H	H			21%
8d	H			H		28%
8e	H			H		29%
8f	H			H		52%
8g	H			H		52%
8h	H			H		39%



156 To resemble the model structure apicidin (1), the nine macrocycles **8a-i** have an aromatic amino
 157 acid at the C-terminal end (R^5) and an adjacent linear alkyl side chain in common (R^3 or R^4). The
 158 peptoid monomer was inserted at the C- or N-terminal position of D-proline (R^1 or R^3). In the latter
 159 case, cyclization was performed on the secondary amine of a peptoid building block, causing a lower
 160 yield on average ($19\% \pm 8$, **8a-c**). Incorporating a peptoid monomer in the middle of the sequence
 161 resulted in overall yields similar to those obtained for cyclic tetrapeptides ($36\% \pm 13$, **8d-i**).

162 Further peptoid building blocks were incorporated into the macrocycles to enhance structural
 163 diversity, resulting in the general structure **9**. Table 3 shows a selection of nine structurally similar
 164 apicidin congeners with both aromatic and aliphatic side chains (Table 3).

165 **Table 3.** Cyclic tetramers of general structure **9** and their respective yields over ten reaction steps.

 9				
Macrocycle	R^1	R^2	R^3	Yield
9a				50%
9b				14%
9c				18%
9d				15%
9e				15%
9f				28%
9g				34%
9h				20%
9i				19%

166 The macrocyclic hybrids **9a-i** are composed of two peptoid monomers (R^1 and R^2) and two amino
 167 acids (d-proline and R^3) located in alternating order on opposite sides of the backbone ring system.
 168 Aromatic and linear, and cyclic aliphatic peptoid monomers built the N-terminus of the linear
 169 precursors (R^1). The individual building blocks did not influence the overall yields, similar to the
 170 yields obtained for hybrids **8a-c** that were also cyclized on a secondary amine ($24\% \pm 11$).

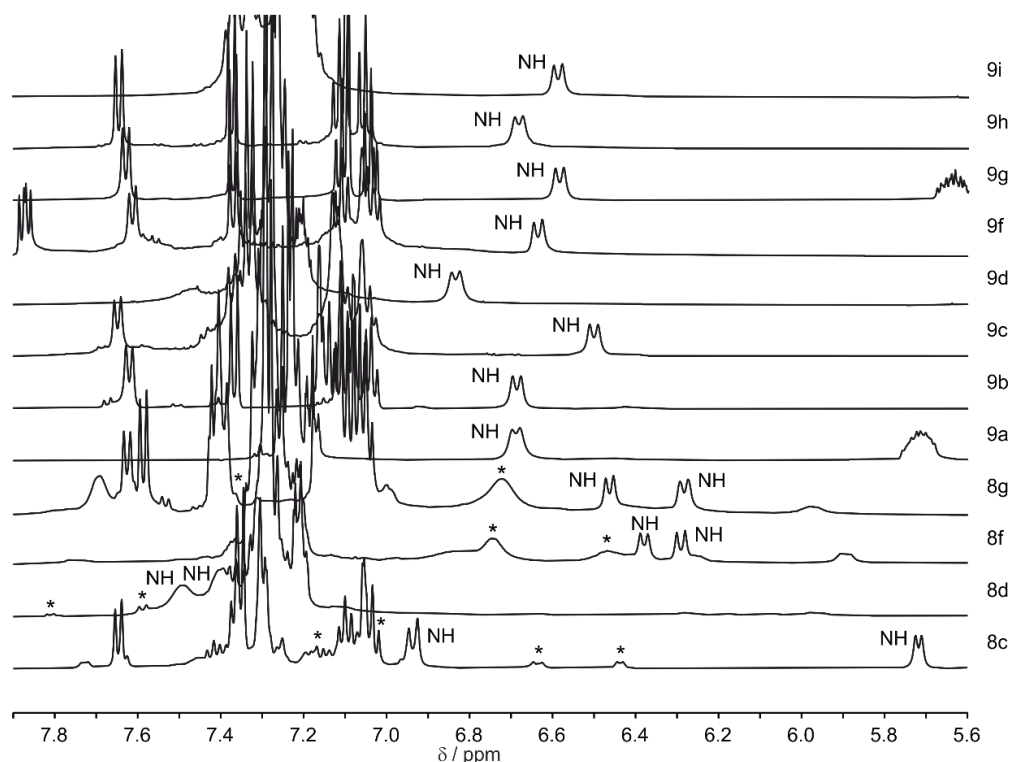
171 2.2. Multiconformational equilibrium detected by NMR

172 Often multiple signal sets are detected in the NMR spectra of macrocycles depending on the
 173 dielectric properties of the solvent [11, 67-69]. This could be due to different conformers present or
 174 conformational equilibrium [20, 70]. Influencing factors are *i.a.* side chains, solvent effects, and
 175 temperature [71, 72]. For the model structure apicidin (1), as an example, it is known that multiple
 176 conformations stem from *cis-trans* isomerism of the pipercolic acid building block [69, 71].

177 HPLC purification of the compounds resulted in sharp peaks indicating that one predominant
178 isomer was synthesized [72-74]. However, NMR-spectra of the cyclic tetramers corroborated the
179 formation of several conformers for almost every macrocycle (supplemental, Table S6). This was most
180 prominent for cyclic tetrapeptides **7a-i**, which tended to assemble in multiconformational equilibria
181 due to multiple degrees of freedom.

182 The same applied to the macrocycles with one peptoid monomer. Macrocycles **8a-i** revealed
183 multiple signal sets in solution, indicating different conformers' formation (supplemental, Table S6).
184 NOESY spectra of macrocycle **8f**, for example, led to the identification of five separate conformers
185 which interconverted on the NMR timescale. Surprisingly, the complexity of the spectra of the
186 hybrids **8a-d** was significantly reduced compared to spectra of structures **8e-i**. The peptoid monomer
187 was inserted at the N-terminus in the former ones, resulting in one dominant structure next to another
188 isomer in approximately 5:1. Therefore, incorporating a peptoid building block in this position could
189 stabilize distinct isomers, decisive for biological applications.

190 For macrocycles **9a-i**, one dominant signal set was mostly observed (supplemental, Table S6). To
191 illustrate this, Figure 3 displays the NH regions of selected macrocycles from series 8 and 9, which
192 were soluble in pure acetonitrile. In the NH region of series 9 macrocycles, only one peptide bond
193 amide signal is visible. For macrocycles **8c**, **8d**, **8f**, and **8g**, one main signal set was accompanied by a
194 second or third signal set of lesser intensity. Macrocycles from series 7 are not shown here, as the
195 molecules were primarily soluble in DMSO (see supplemental, Table S6).

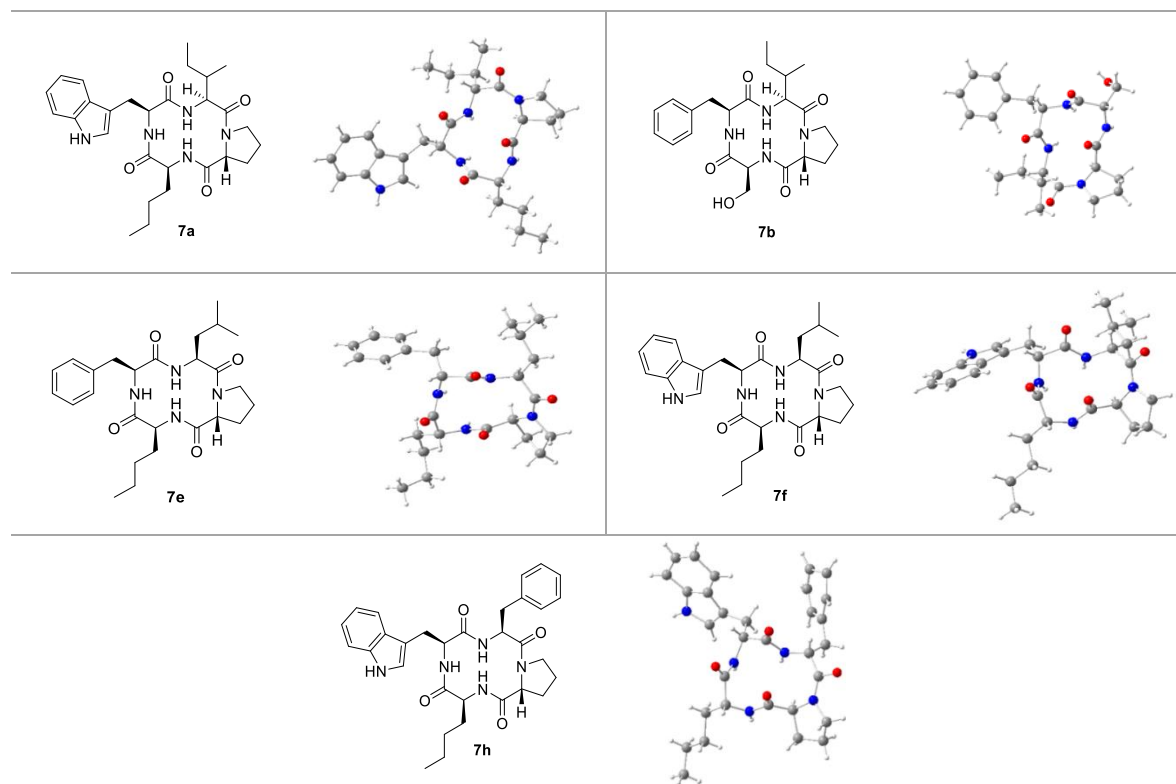


196 **Figure 3:** Excerpts from ^1H spectra of selected macrocycles from series 8 and 9. An asterisk (*) indicates
197 the NH signals belonging to a signal set of lower intensity. The spectra were normalized to have
198 similar NH intensity.

199

200 2.3. Spatial structure in solid-state

201 X-ray diffraction is a highly reliable method to determine the spatial structure of molecules in
202 the solid-state [75, 76]. Crystallization of the macrocyclic hybrids was attempted *via* evaporation of
203 acetonitrile, isopropanol, and methanol. Most macrocycles aggregated into amorphous powders
204 during this process, some became viscous oils, and others produced polycrystalline needle-shaped
205 structures. However, some single crystals were obtained from multiple attempts for each of the five
206 similar cyclic tetrapeptides **7a**, **7b**, **7e**, **7f**, and **7h** (Figure 4).

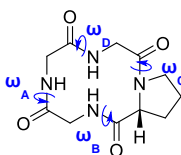


207 **Figure 4:** Molecular structure of the cyclic tetrapeptides **7a** and **7b** and one of the independent
208 crystallographic molecules of macrocycles **7e**, **7f**, and **7h**.

209 Macrocycle **7b** represents the only tetrapeptide with a polar building block crystallized in
210 sufficient quality for X-ray diffraction. In contrast to the other structures, **7b** is equipped with L-serine
211 instead of the alkyl side chain L-norleucine. Thus, the macrocycle **7b** is the only member of the
212 apicidin tetrapeptide library without L-norleucine that crystallized upon vapor diffusion.

213 For both tetrapeptides **7a** and **7b** containing an *N*-terminal L-isoleucyl residue, the structure of
214 one isomer was determined *via* X-ray diffraction. As for the model structure apicidin (**1**) [69], at least
215 three independent structures (I, II, III etc.) each were obtained for macrocycles **7e**, **7f**, and **7h**. Their
216 dihedral angles differ slightly from each other but show the same *cis-trans* arrangement (Table 4).

217

218
219**Table 4:** Dihedral angles of the independent structures of macrocycles **7a**, **7b**, **7e**, **7f**, and **7h** determined *via* X-ray diffraction measurements.

Macrocycle	Structure	ω_A	ω_B	ω_C	ω_D
7a	I	155.7°	171.1°	5.2°	-167.6°
7b	I	159.0°	171.5°	6.5°	-172.7°
7e	I	157.3°	170.1°	12.1°	-173.3°
	II	158.1°	169.5°	6.5°	-172.4°
	III	158.5°	171.8°	13.1°	-175.6°
7f	I	160.4°	167.9°	-3.7°	-172.6°
	II	160.8°	167.4°	13.6°	-174.4°
	III	163.3°	166.8°	9.8°	-174.8
	IV	165.5°	163.7°	14.6°	-177.6°
	V	165.3°	163.9°	10.9°	-177.0°
7h	I	157.9°	169.0°	5.0°	-170.6°
	II	157.1°	169.6°	-6.9°	-168.0°
	III	153.1°	169.6°	13.5°	-172.7°
	IV	155.3°	171.0°	3.1°	-165.6°

220

To elucidate the backbone conformation, dihedral angles of the individual macrocycles were measured. The dihedral angle ω describes the torsion angle of the axis between the α - and the amide carbon atom of one amino acid and the axis between the amide nitrogen and the α -carbon atom of the following building block. Due to the partial double-bond character of the peptide bond, this angle is forced into two distinct values: $\omega = 0^\circ$ or $\omega = \pm 180^\circ$. Sterical hindrance can lead to a deviation of the dihedral angles from their ideal values, but an angle close to $\omega = 0^\circ$ indicates a *cis*-conformation while $\omega = \pm 180^\circ$ indicates a *trans*-peptide bond [77].

227

All conformers of the five macrocycles **7a**, **7b**, **7e**, **7f**, and **7h** showed a *cis*-conformation between the nitrogen atom of their respective D-prolyl residue and the amide carbon of the adjacent amino acid (ω_C). The *trans-trans-cis-trans* sequence of the backbone has also been reported for the model structure apicidin (**1**) [69] and similar cyclotetrapeptides [78]. The largest deviations from the ideal dihedral angle were measured between the nitrogen atoms of the large aromatic side chains L-phenylalanine or L-tryptophan and the amide carbon of the following building blocks (ω_A).

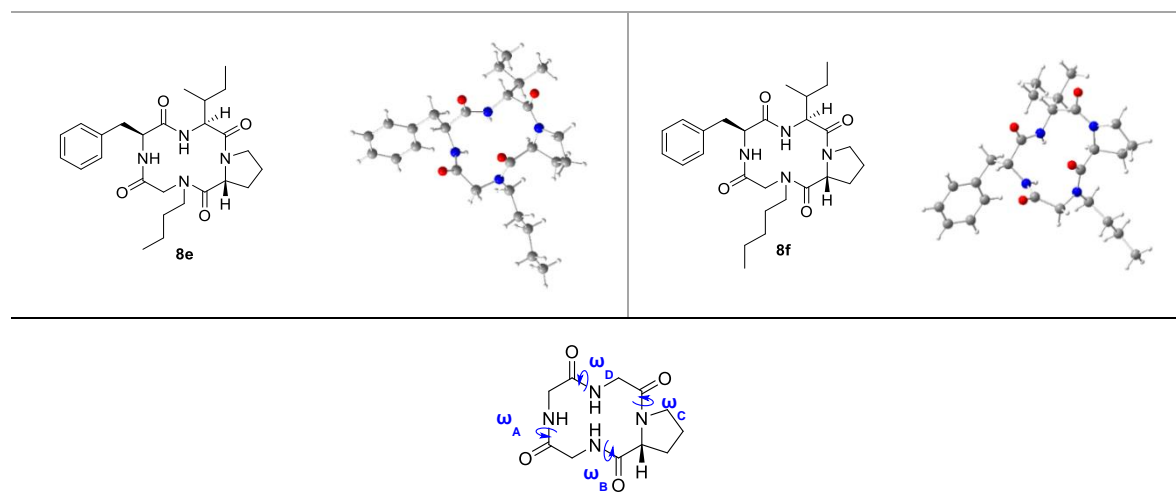
233

The measurements of the configurations of the α -carbon atoms showed the expected stereochemistry: the α -carbon of every D-proline building block was (*R*)-, the ones of the remaining amino acids were (*S*)-configured. Furthermore, the macrocycles resembled each other in the location of their side chains: while the aliphatic ring of D-proline pointed above the ring level, the remaining side chains were located below.

238

Crystallization preparations of hybrids containing one peptoid monomer provided single crystals of two compounds: **8e** and **8f** (Table 5). Both revealed strong structural similarities to the cyclic tetrapeptides **7a-i**. Moreover, the macrocycles **8e** and **8f** are equivalent to each other in large parts of their structure but differ in their peptoid-based alkyl side chain length.

242

243
244**Table 5:** Molecular structures of the cyclic hybrids **8e** and **8f** and their dihedral angles determined *via* X-ray diffraction measurements.


Macrocycle	ω_A	ω_B	ω_C	ω_D
8e	155.2°	169.4°	12.2°	-173.0°
8f	155.3°	170.7°	13.5°	-172.4°

245
246
247
248
249
250
251
252

The dihedral angles of the peptide-peptoid hybrids resemble the ones measured for cyclic tetrapeptides. Again, a *cis*-conformation was measured between the nitrogen atom of D-proline and the amide carbon of the following building block. As for tetrapeptides of general structure **7**, three residues were located on the same side of the ring plane while the alkyl ring of D-proline pointed towards the opposite direction.

We could not successfully crystallize any cyclic hybrid of compounds with two peptoid units (series **9**). Thus, we decided to use NMR data for the structure elucidation of the exemplarily chosen macrocycle **9a**.

253

2.4. Spatial structure in solution state

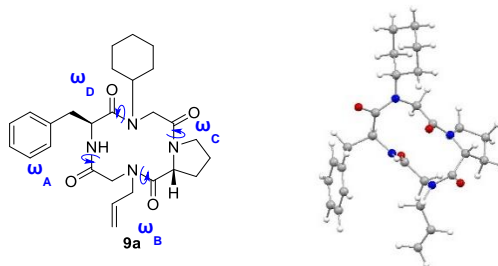
254
255
256
257
258
259
260
261
262
263
264
265
266
267
268
269
270
271
272
273
274
275

Structural information on **9a** was obtained by recording NOESY spectra. Internuclear distances were calculated from NOE cross-peak intensities (see supplemental, Table S2 for details). Using the internuclear distance data from NOESY spectra and dihedral angle information from *J*-coupling constants, a 3D model for **9a** was constructed with the molecular modeling software Avogadro (<http://avogadro.cc>) [79]. This model was further structurally optimized utilizing a DFT approach using the quantum chemical calculation software Turbomole (<http://www.turbomole.com>).

However, NOE data of small molecules is often not sufficient to unambiguously select for one conformation, especially in structural backbone dynamics. Additional structural information regarding **9a** was obtained by extraction of one- and two-bond residual dipolar couplings (RDCs) in a uniaxially stretched polyethylene glycol (PEG) gel [80]. This was achieved by recording CLIP-HSQC [81] and P.E.HSQC [82] spectra of the molecule in an isotropic environment and under anisotropic conditions in a uniaxially stretched polyethylene glycol (PEG) gel [80]. The RDCs were then used to validate the NOE-derived structure. To assess whether the RDCs agree with the constructed model, they were analyzed using single value decomposition (SVD) in the MSpin-RDC software [83]. An SVD omitting the RDC data of the more mobile sidechains yielded acceptable results. The back-calculated and experimental RDCs were in good agreement, with 7 out of 8 RDCs fulfilled within the experimental error (supplemental, Table S3). A full back-calculation including sidechain RDCs can be found in the supporting information (supplemental, Table S3). Although the deviation between experimental and back-calculated values was higher in this case, all RDC values were reasonably well reproduced. The constructed model is therefore largely in agreement with the experimental NOE, *J*-coupling, and RDC data and can be seen to represent the dominant solution state structure of **9a**.

276 The 3D model of **9a** indicated interesting structural differences compared to the macrocycles
277 with three or four amino acids (Table 6).

278 **Table 6:** Dihedral angles and molecular solution-state structure of the macrocycle **9a** determined *via*
279 NMR measurements.



Macrocycle	ω_A	ω_B	ω_C	ω_D
9a	-179.3°	14.8°	-177.1°	-11.2°

280 The model of **9a** displays an alternating *cis-trans*-configuration of the cyclic backbone and an
281 overall oblong ring shape. Thereby, the torsion angles ω_A and ω_C indicate a *trans*-peptide bond
282 between the amino functions of both amino acids and the carbonyl moieties of the subsequent
283 peptoid monomers. In contrast to previous structures, no *cis*-bond was measured between the
284 nitrogen atom of proline and the amide carbon of the following building block (ω_C). Instead, two *cis*-
285 bonds were detected between the nitrogen atoms of the peptoid monomers and the subsequent
286 carbonyl carbon atoms (ω_B and ω_D). Likewise, the dihedral angle ω_A next to the sterically demanding
287 side chains of L-phenylalanine was no longer distorted from ideal values ($\omega_A = 179.3^\circ$). Previous
288 studies on small cyclic peptoids have shown that the *cis-trans-cis-trans* arrangement represents the
289 lowest energy conformation and forms during the crystallization process of different cyclic
290 tetrapeptoids [84-86]. Our data indicate that this characteristic backbone arrangement is also favored
291 in cyclic hybrids of general structure **9**. Thus, with an increase in the peptide-peptoid ratio, the
292 backbone configuration of apicidin derivatives can be easily modified.

293 Besides backbone configuration, the side chains of **9a** differed from previous derivatives: the
294 side chains were located alternately above and below the ring plane. This characteristic orientation is
295 also known for pure peptoid macrocycles of different ring sizes [23, 84, 85] and various *N*-alkylated
296 tetrapeptides [87-92].

297 Our data indicate that the increase of the peptoid-to-peptide ratio leads to significant structural
298 changes of the entire macrocycle, which must be considered when developing potential inhibitors of
299 the Wnt/ β -catenin pathway.

300 3. Materials and Methods

301 **General procedure for the synthesis of cyclic peptoids:** In a fritted syringe, a 2-chlorotrityl-
302 chloride resin (125 mg, 200 μmol , 1.60 mmol/mg loading density, 100–200 mesh, 1.00 equiv.) was
303 swollen in methylene chloride (DCM) for at least 30 min at 21 $^\circ\text{C}$. After filtration, either a freshly
304 prepared solution of bromoacetic acid (8.00 equiv.) and *N,N'*-diisopropylethylamine (DIPEA,
305 8.00 equiv.) in *N,N'*-dimethyl-formamide (DMF) or a Fmoc-protected amino acid (4.00 equiv.) and
306 DIPEA (4.00 equiv.) in *N*-methylpyrrolidone (NMP) was added and shaken for 1 h or rather 16 h at
307 21 $^\circ\text{C}$. The resin was extensively washed with DMF, methanol, and DCM. In the former case, a
308 solution of the corresponding amine (8.00 equiv.) in DMF was added to the resin and shaken for 1 h
309 at 21 $^\circ\text{C}$. In the latter case, a solution of 20% piperidine in DMF was repeatedly added. Following
310 extensive washing, either a solution of bromoacetic acid (8.00 equiv.) and *N,N'*-diisopropyl-
311 carbodiimide (DIC, 8.00 equiv.) in DMF or a Fmoc-protected amino acid (4.00 equiv.),
312 1-hydroxybenzotriazole (HOBt, 4.00 equiv.) and DIC (4.00 equiv.) in NMP were added and shaken
313 for 30 min or 4 h at 21 $^\circ\text{C}$. Substitution or rather Fmoc-deprotection and acetylation or rather amino

314 acid coupling were alternated repeatedly until the desired tetramer was built. For cleavage, a solution
315 of 33% hexafluoroisopropanol in DCM was added, and the mixture was shaken overnight. The
316 solvent was removed under an air stream.

317 For the cyclization, a solution of the respective linear tetramer was added dropwise to a solution
318 of [dimethylamino(triazolo[4,5-b]pyridin-3-yloxy)-methylidene]-dimethylazanium hexafluoro-
319 phosphate (HATU, 1.50 equiv.) and DIPEA (8.00 equiv.) in DMF. The mixture was stirred overnight
320 at 21 °C, and the solvent was removed under reduced pressure. The residue was purified *via*
321 preparative reversed-phase HPLC.

322 **Crystal structure determination:** The single-crystal X-ray diffraction studies were carried out on
323 a Bruker D8 Venture diffractometer with a PhotonII detector at 123(2) K, 173(2) K, or 298(2) K using
324 Cu-K α radiation ($\lambda = 1.54178 \text{ \AA}$). Dual space methods (SHELXT) [93] were used for structure solution,
325 and refinement was carried out using SHELXL (full-matrix least-squares on F^2) [94]. Hydrogen atoms
326 were localized by difference electron density determination and refined using a riding model (H(N,
327 O) free). Semi-empirical absorption corrections were applied. For **7a** and **8e**, extinction corrections
328 were applied. The absolute configuration was determined for all structures refinement of Parsons' χ -
329 parameter [95]. For disorder, restraints, constraints, and SQUEEZE, see the corresponding cif-files for
330 details. CCDC 2059042 (**7a**), 2059043 (**7f**), 2059044 (**7e**), 2059045 (**8f**), 2059047 (**7h**), 2059048 (**8e**), and
331 2059049 (**7b**) contain the supplementary crystallographic data for this paper. These data can be
332 obtained free of charge from The Cambridge Crystallographic Data Centre *via*
333 www.ccdc.cam.ac.uk/data_request/cif.

334 **NMR measurements:** NMR spectra were recorded at 25 °C on an Avance 300 (Bruker BioSpin,
335 Germany) and a Bruker Avance 500 spectrometer. Additional NMR spectra of peptide-peptoid
336 hybrid **9a** were recorded at 30 °C on a 600 MHz Avance III spectrometer with a TCI cryo-probe head
337 (Bruker BioSpin, Germany). More details on the NMR measurements can be found in the
338 supplementary information.

339 4. Conclusions

340 The three different classes of tetrameric cyclic peptide-peptoid hybrids presented here will pave
341 the way to further research on this promising class of compounds. All macrocycles were designed to
342 resemble the fungal metabolite apicidin (**1**) but without the characteristic Aoda side chain, critical for
343 its literature known HDAC inhibitor activity [46]. The cyclic tetramers are accessible in moderate
344 yields by combining different solid-phase techniques followed by ring closure in solution.

345 Several studies had previously shown that cyclic tetramers might adopt multiple conformations
346 in solution, especially interchanging *cis* and *trans* peptide bonds [7, 11, 70]. The active conformation
347 of biologically potent molecules in solution may be selected in reality from various interconverting
348 conformers. The stability of the single conformers depends on intra- as well as intermolecular
349 interactions [72]. The conversion rate between these conformers is quite high, making it difficult to
350 identify every isomer formed [71, 72].

351 Our X-ray and NMR measurements revealed the formation of different isomers in solid and
352 liquid states for the cyclic tetramers presented. The amount of conformational variability depended
353 on the number of incorporated peptoid units. Solution state NMR spectroscopy indicated different
354 conformers for all compounds that exchanged partially within the NMR time scale. Especially for
355 macrocycles with no or one peptoid monomer, multiple signal sets were detected. The incorporation
356 of two peptoid monomers led to the stabilization of one dominant isomer.

357 Crystallographically detected conformers differed only in details concerning the backbone
358 structure of the cyclic ring. Tetrapeptide conformers varied slightly in their dihedral angles but
359 showed the same *cis-trans* sequence. The incorporation of one peptoid monomer did not change this
360 *cis-trans* arrangement. The insertion of two peptoid monomers significantly affected the overall
361 conformation. Instead of one, two *cis*-bonds were detected in the resulting macrocycles, indicating
362 that the amount of peptoid monomers influences the spatial structure of peptide-peptoid hybrids.

363 With the structural information now in hand, biological targets can be identified, and, thanks to
364 the modular approach, highly specific hybrids can be easily synthesized. These new molecules will
365 find application in biochemical and medical research and help elucidate and sustain life's complexity.
366 We will continue our work on the activity of our macrocycles towards the Wnt/ β -catenin signaling
367 pathway. So far, we have found some hybrids with inhibition constants in the range of the model
368 structure apicidin (**1**, data not shown). The structural investigations reported herein will help us
369 design different potent inhibitors of the Wnt/ β -catenin pathway, a signaling cascade involved in
370 embryogenesis and homeostasis, and different diseases such as cancer or neurodegenerative
371 disorders [96-102].

372 **Supplementary Materials:** The following are available online: synthetic procedure, crystallographic, and NMR
373 data.

374 **Author Contributions:** Conceptualization, C.N.H., and A.S.; methodology, C.N.H., A.S., T.G. and C.M.-G.;
375 validation, C.M.-G., and S.B.; formal analysis, C.N.H., A.S., T.G., M.N. and C.M.-G.; investigation, C.N.H., A.S.,
376 J.B. and L.C.S.; resources, C.M.-G. and S.B.; data curation, C.N.H., A.S., J.B., L.C.S., and M.N.; writing—original
377 draft preparation, C.N.H., and A.S.; writing—review and editing, C.M.-G., T.G., and S.B.; visualization, C.N.H.,
378 A.S.; supervision, C.M.-G., and S.B.; project administration, C.M.-G., and S.B.; funding acquisition, C.M.-G., and
379 S.B.. All authors have read and agreed to the published version of the manuscript.

380 **Funding:** This research received no external funding.

381 **Acknowledgments:** We acknowledge support from the KIT and the DFG (GRK2039). C.M.-G. acknowledges
382 funding by the Helmholtz-Society. We thank Ansgar Pausch, KIT, to help Turbomole and Prof. Wim Klopper
383 and Dr. Sebastian Höfener, KIT, provide access to the TCHCLX400 cluster.

384 **Conflicts of Interest:** The authors declare no conflict of interest.

385 References

- 386 1. Beatriz, G., Albericio, F., *Molecules*, 2020, **25**(10).
- 387 2. Lee, A. C.-L., Harris, J. L., Khanna, K. K., Hong, J.-H., *Int. J. Mol. Sci.*, 2019, **20**(10), 2383.
- 388 3. Zhang, Y., Zhang, H., Ghosh, D., Williams III, R. O., *Int. J. Pharm.*, 2020, 119491.
- 389 4. Drucker, D. J., *Nat. Rev. Drug Discov.*, 2019, 1-13.
- 390 5. Zorzi, A., Deyle, K., Heinis, C., *Curr. Opin. Chem. Biol.*, 2017, **38**, 24-29.
- 391 6. Choi, J.-S., Joo, S. H., *Biomol. Ther. (Seoul)*, 2020, **28**(1), 18.
- 392 7. Horton, D. A., Bourne, G. T., Coughlan, J., Kaiser, S. M., Jacobs, C. M., Jones, A., Rühmann, A., Turner,
393 J. Y., Smythe, M. L., *Org. Biomol. Chem.*, 2008, **6**(8), 1386-1395.
- 394 8. Meutermans, W. D., Bourne, G. T., Golding, S. W., Horton, D. A., Campitelli, M. R., Craik, D., Scanlon,
395 M., Smythe, M. L., *Org. Lett.*, 2003, **5**(15), 2711-2714.
- 396 9. Sarojini, V., Cameron, A. J., Varnava, K. G., Denny, W. A., Sanjayan, G., *Chem. Rev.*, 2019, **119**(17), 10318-
397 10359.
- 398 10. Davison, E. K., Cameron, A. J., Harris, P. W., Brimble, M. A., *MedChemComm*, 2019, **10**(5), 693-698.
- 399 11. Ferracane, M. J., Brice-Tutt, A. C., Coleman, J. S., Simpson, G. G., Wilson, L. L., Eans, S. O., Stacy, H. M.,
400 Murray, T. F., McLaughlin, J. P., Aldrich, J. V., *ACS Chem. Neurosci.*, 2020, **11**(9), 1324-1336.
- 401 12. Betancur, L. A., Forero, A. M., Romero-Otero, A., Sepúlveda, L. Y., Moreno-Sarmiento, N. C.,
402 Castellanos, L., Ramos, F. A., *J. Antibiot. Res.*, 2019, **72**(10), 744-751.
- 403 13. Grauer, A., König, B., *Eur. J. Org. Chem.*, 2009, **2009**(30), 5099-5111.
- 404 14. Ko, E., Liu, J., Perez, L. M., Lu, G., Schaefer, A., Burgess, K., *J. Am. Chem. Soc.*, 2011, **133**(3), 462-477.
- 405 15. Zuckermann, R. N., Kerr, J. M., Kent, S. B., Moos, W. H., *J. Am. Chem. Soc.*, 1992, **114**(26), 10646-10647.
- 406 16. Sun, J., Zuckermann, R. N., *ACS nano*, 2013, **7**(6), 4715-4732.
- 407 17. Zuckermann, R. N., Kodadek, T., *Curr. Opin. Mol. Ther.*, 2009, **11**(3), 299-307.

- 408 18. Dohm, M. T., Kapoor, R., Barron, A. E., *Curr. Pharm. Des.*, 2011, **17**(25), 2732-2747.
- 409 19. Yoo, B., Kirshenbaum, K., *Curr. Opin. Chem. Biol.*, 2008, **12**(6), 714-721.
- 410 20. De Riccardis, F., *Eur. J. Org. Chem.*, 2020, **2020**(20), 2981-2994.
- 411 21. Butterfoss, G. L., Renfrew, P. D., Kuhlman, B., Kirshenbaum, K., Bonneau, R., *J. Am. Chem. Soc.*, 2009,
412 **131**(46), 16798-16807.
- 413 22. Shin, S. B., Yoo, B., Todaro, L. J., Kirshenbaum, K., *J. Am. Chem. Soc.*, 2007, **129**(11), 3218-3225.
- 414 23. Yoo, B., Shin, S. B. Y., Huang, M. L., Kirshenbaum, K., *Chem. Eur. J.*, 2010, **16**(19), 5528-5537.
- 415 24. Vollrath, S. B., Hu, C., Bräse, S., Kirshenbaum, K., *Chem. Commun.*, 2013, **49**(23), 2317-2319.
- 416 25. Webster, A. M., Cobb, S. L., *Chem. Eur. J.*, 2018, **24**(30), 7560-7573.
- 417 26. Vollrath, S. B., Bräse, S., Kirshenbaum, K., *Chem Sci.*, 2012, **3**(9), 2726-2731.
- 418 27. Herlan, C. N., Sommer, K., Weis, P., Nieger, M., Bräse, S., *Molecules*, 2021, **26**(1), 150.
- 419 28. D'Amato, A., Pierri, G., Tedesco, C., Della Sala, G., Izzo, I., Costabile, C., De Riccardis, F., *J. Org. Chem.*,
420 2019, **84**(17), 10911-10928.
- 421 29. Tedesco, C., Erra, L., Izzo, I., De Riccardis, F., *CrystEngComm*, 2014, **16**(18), 3667-3687.
- 422 30. Biron, E., Chatterjee, J., Kessler, H., *J. Pept. Sci.*, 2006, **12**(3), 213-219.
- 423 31. Chatterjee, J., Gilon, C., Hoffman, A., Kessler, H., *Acc. Chem. Res.*, 2008, **41**(10), 1331-1342.
- 424 32. Demmer, O., Dijkgraaf, I., Schottelius, M., Wester, H.-J., Kessler, H., *Org. Lett.*, 2008, **10**(10), 2015-2018.
- 425 33. Titlestad, K., Schwitters, B., Sundholm, F., *Acta Chem. Scand. B*, 1977, **31**(8), 641-661.
- 426 34. Wessjohann, L. A., Andrade, C. K. Z., Vercillo, O. E., Rivera, D. G., *Targets Heterocycl. Syst.*, 2006, **10**, 24-
427 53.
- 428 35. Morimoto, J., Kodadek, T., *Mol. Biosyst.*, 2015, **11**(10), 2770-2779.
- 429 36. Olsen, C. A., *ChemBioChem*, 2010, **11**(2), 152-160.
- 430 37. Olsen, C. A., Montero, A., Leman, L. J., Ghadiri, M. R., *ACS Med. Chem. Lett.*, 2012, **3**(9), 749-753.
- 431 38. Boehm, M., Beaumont, K., Jones, R., Kalgutkar, A. S., Zhang, L., Atkinson, K., Bai, G., Brown, J. A., Eng,
432 H., Goetz, G. H., Holder, B. R., Khunte, B., Lazzaro, S., Limberakis, C., Ryu, S., Shapiro, M. J., Tylaska,
433 L., Yan, J., Turner, R., Leung, S. S. F., Ramaseshan, M., Price, D. A., Liras, S., Jacobson, M. P., Earp, D.
434 J., Lokey, R. S., Mathiowetz, A. M., Menhaji-Klotz, E., *J. Med. Chem.*, 2017, **60**(23), 9653-9663.
- 435 39. Greco, I., Emborg, A. P., Jana, B., Molchanova, N., Oddo, A., Damborg, P., Guardabassi, L., Hansen, P.
436 R., *Scientific reports*, 2019, **9**(1), 1-12.
- 437 40. Hansen, A. M., Skovbakke, S. L., Christensen, S. B., Perez-Gassol, I., Franzyk, H., *Amino Acids*, 2019,
438 **51**(2), 205-218.
- 439 41. Frederiksen, N., Hansen, P. R., Björkling, F., Franzyk, H., *Molecules*, 2019, **24**(24), 4429.
- 440 42. Singh, S. B., Zink, D. L., Polishook, J. D., Dombrowski, A. W., Darkin-Rattray, S. J., Schmatz, D.
441 M., Goetz, M. A., *Tetrahedron Lett.*, 1996, **37**(45), 8077-8080.
- 442 43. Darkin-Rattray, S. J., Gurnett, A. M., Myers, R. W., Dulski, P. M., Crumley, T. M., Allocco, J. J., Cannova,
443 C., Meinke, P. T., Colletti, S. L., Bednarek, M. A., *PNAS USA*, 1996, **93**(23), 13143-13147.
- 444 44. Colletti, S. L., Myers, R. W., Darkin-Rattray, S. J., Gurnett, A. M., Dulski, P. M., Galuska, S., Allocco, J.
445 J., Ayer, M. B., Li, C., Lim, J., *Bioorg. Med. Chem. Lett.*, 2001, **11**(2), 107-111.
- 446 45. Meinke, P. T., Colletti, S. L., Ayer, M. B., Darkin-Rattray, S. J., Myers, R. W., Schmatz, D. M., Wyvratt,
447 M. J., Fisher, M. H., *Tetrahedron Lett.*, 2000, **41**(41), 7831-7835.
- 448 46. Singh, S. B., Zink, D. L., Liesch, J. M., Mosley, R. T., Dombrowski, A. W., Bills, G. F., Darkin-Rattray, S.
449 J., Schmatz, D. M., Goetz, M. A., *J. Org. Chem.*, 2002, **67**(3), 815-825.
- 450 47. Grathwohl, C., Wüthrich, K., *Biopolymers*, 1981, **20**(12), 2623-2633.

- 451 48. Fischer, G., *Chem. Soc. Rev.*, 2000, **29**(2), 119-127.
- 452 49. Schubert, M., Labudde, D., Oschkinat, H., Schmieder, P., *J. Biomol. NMR*, 2002, **24**(2), 149-154.
- 453 50. Mathieu, S., Poteau, R., Trinquier, G., *J. Phys. Chem. B*, 2008, **112**(26), 7894-7902.
- 454 51. Scherer, G., Kramer, M. L., Schutkowski, M., Reimer, U., Fischer, G., *J. Am. Chem. Soc.*, 1998, **120**(22),
455 5568-5574.
- 456 52. Wedemeyer, W. J., Welker, E., Scheraga, H. A., *Biochemistry*, 2002, **41**(50), 14637-14644.
- 457 53. Krieger, F., Möglich, A., Kiefhaber, T., *J. Am. Chem. Soc.*, 2005, **127**(10), 3346-3352.
- 458 54. Fairweather, K. A., Sayyadi, N., Luck, I. J., Clegg, J. K., Jolliffe, K. A., *Org. Lett.*, 2010, **12**(14), 3136-3139.
- 459 55. Rodriguez, L. M. D. L., Weitkamp, A. J., Brimble, M. A., *Org. Biomol. Chem.*, 2015, **13**(25), 6906-6921.
- 460 56. Merrifield, R. B., *J. Am. Chem. Soc.*, 1963, **85**(14), 2149-2154.
- 461 57. Zuckermann, R. N., Kerr, J. M., Kent, S. B. H., Moos, W. H., *J. Am. Chem. Soc.*, 1992, **114**(26), 10646-10647.
- 462 58. Aldrich, J. V., Kulkarni, S. S., Senadheera, S. N., Ross, N. C., Reilley, K. J., Eans, S. O., Ganno, M. L.,
463 Murray, T. F., McLaughlin, J. P., *ChemMedChem*, 2011, **6**(9), 1739-1745.
- 464 59. Dahiya, R., Gautam, H., *Mar. Drugs*, 2011, **9**(1), 71-81.
- 465 60. El-Faham, A., Albericio, F., *Chem. Rev.*, 2011, **111**(11), 6557-6602.
- 466 61. Thakkar, A., Trinh, T. B., Pei, D., *ACS Comb. Sci.*, 2013, **15**(2), 120-129.
- 467 62. Wong, C. T., Lam, H. Y., Song, T., Chen, G., Li, X., *Angew. Chem. Int. Ed.*, 2013, **52**(39), 10212-10215.
- 468 63. Pedroso, E., Grandas, A., de las Heras, X., Eritja, R., Giralte, E., *Tetrahedron Lett.*, 1986, **27**(6), 743-746.
- 469 64. Gisin, B. F., Merrifield, R., *J. Am. Chem. Soc.*, 1972, **94**(9), 3102-3106.
- 470 65. Kirshenbaum, K., Barron, A. E., Goldsmith, R. A., Armand, P., Bradley, E. K., Truong, K. T., Dill, K. A.,
471 Cohen, F. E., Zuckermann, R. N., *Proc. Natl. Acad. Sci. U. S. A.*, 1998, **95**(8), 4303-4308.
- 472 66. Zuckermann, R. N., *J. Pept. Sci.*, 2011, **96**(5), 545-555.
- 473 67. Rich, D. H., Kawai, M., Jasensky, R. D., *Int. J. Pept. Protein Res.*, 1983, **21**(1), 35-42.
- 474 68. Merten, C., Li, F., Bravo-Rodriguez, K., Sanchez-Garcia, E., Xu, Y., Sander, W., *PCCP*, 2014, **16**(12), 5627-
475 5633.
- 476 69. Kranz, M., Murray, P. J., Taylor, S., Upton, R. J., Clegg, W., Elsegood, M. R., *J. Pept. Sci.*, 2006, **12**(6), 383-
477 388.
- 478 70. Kessler, H., *Angew. Chem. Int. Ed.*, 1982, **21**(7), 512-523.
- 479 71. Horne, W. S., Olsen, C. A., Beierle, J. M., Montero, A., Ghadiri, M. R., *Angew. Chem. Int. Ed.*, 2009, **48**(26),
480 4718-4724.
- 481 72. Aberhart, D. J., Cotting, J.-A., Lin, H.-J., *Anal. Biochem.*, 1985, **151**(1), 88-91.
- 482 73. Soukup-Hein, R. J., Schneiderheinze, J., Mehelic, P., Armstrong, D. W., *Chromatographia*, 2007, **66**(7), 461-
483 468.
- 484 74. Huang, Y., Pan, L., Zhao, L., Mant, C. T., Hodges, R. S., Chen, Y., *Biomed. Chromatogr.*, 2014, **28**(4), 511-
485 517.
- 486 75. Chruszcz, M., Borek, D., Domagalski, M., Otwinowski, Z., Minor, W., *X-ray diffraction experiment: The*
487 *last experiment in the structure elucidation process*, in *Adv. Protein Chem. Struct. Biol.* 2009, Elsevier. p. 23-
488 40.
- 489 76. Garman, E. F., *Science*, 2014, **343**(6175), 1102-1108.
- 490 77. Ramachandran, G., Chandrasekaran, R., Kopple, K. D., *Biopolymers*, 1971, **10**(11), 2113-2131.
- 491 78. Nakai, H., Nagashima, K., Itazaki, H., *Acta Crystallogr. Sect. C: Cryst. Struct. Commun.*, 1991, **47**(7), 1496-
492 1499.

- 493 79. Hanwell, M. D., Curtis, D. E., Lonie, D. C., Vandermeersch, T., Zurek, E., Hutchison, G. R., J.
494 *Cheminformatics*, 2012, **4**(1), 1-17.
- 495 80. Gloge, T., *Development of a universal alignment medium for the extraction of RDCs and structure elucidation*
496 *with tensorial constraints*. 2020, Karlsruhe University of Technology.
- 497 81. Enthart, A., Freudenberger, J. C., Furrer, J., Kessler, H., Luy, B., *J. Magn. Reson.*, 2008, **192**(2), 314-322.
- 498 82. Tzvetkova, P., Simova, S., Luy, B., *J. Magn. Reson.*, 2007, **186**(2), 193-200.
- 499 83. Navarro-Vázquez, A., *Magn. Reson. Chem.*, 2012, **50**(S1), S73-S79.
- 500 84. Culf, A. S., Cuperlović-Culf, M., Leger, D. A., Decken, A., *Org. Lett.*, 2014, **16**(10), 2780-2783.
- 501 85. Caumes, C., Fernandes, C., Roy, O., Hjelmgaard, T., Wenger, E., Didierjean, C., Taillefumier, C., Faure,
502 S., *Org. Lett.*, 2013, **15**(14), 3626-3629.
- 503 86. Maulucci, N., Izzo, I., Bifulco, G., Aliberti, A., De Cola, C., Comegna, D., Gaeta, C., Napolitano, A.,
504 Pizza, C., Tedesco, C., *Chem. Commun.*, 2008(33), 3927-3929.
- 505 87. Dale, J., Titlestad, K., *J. Chem. Soc. D*, 1970(21), 1403-1404.
- 506 88. Märtle, W., Link, U., Witschel, W., Thewalt, U., Weber, T., Rothe, M., *Biopolymers*, 1991, **31**(6), 735-744.
- 507 89. Seebach, D., Bezençon, O., Jaun, B., Pietzonka, T., Matthews, J. L., Kühnle, F. N., Schweizer, W. B., *Helv.*
508 *Chim. Acta*, 1996, **79**(3), 588-608.
- 509 90. Swepston, P. N., Cordes, A., Kuyper, L., Meyer, W. L., *Acta Crystallogr. B*, 1981, **37**(5), 1139-1141.
- 510 91. Loiseau, N., Gomis, J. M., Santolini, J., Delaforge, M., André, F., *Biopolymers*, 2003, **69**(3), 363-385.
- 511 92. Chiang, C. C., Karle, I. L., *Int. J. Pept. Protein Res.*, 1982, **20**(2), 133-138.
- 512 93. Sheldrick, G., *Acta Crystallogr. B*, 2015, **71**(1), 3-8.
- 513 94. Sheldrick, G. M., *Acta Crystallogr. C*, 2015, **71**(1), 3-8.
- 514 95. Parsons, S., Flack, H. D., Wagner, T., *Acta Crystallogr. B*, 2013, **69**(3), 249-259.
- 515 96. Logan, C. Y., Nusse, R., *Annu. Rev. Cell Dev. Biol.*, 2004, **20**, 781-810.
- 516 97. Huelsken, J., Behrens, J., *J. Cell Sci.*, 2002, **115**(21), 3977-3978.
- 517 98. Hoffmeyer, K., Raggioli, A., Rudloff, S., Anton, R., Hierholzer, A., Del Valle, I., Hein, K., Vogt,
518 R., Kemler, R., *Science*, 2012, **336**(6088), 1549-1554.
- 519 99. Niehrs, C., *Nat. Rev. Mol. Cell Biol.*, 2012, **13**(12), 767-779.
- 520 100. Inestrosa, N. C., Arenas, E., *Nat. Rev. Neurosci.*, 2010, **11**(2), 77-86.
- 521 101. Cisternas, P., Henriquez, J. P., Brandan, E., Inestrosa, N. C., *Mol. Neurobiol.*, 2014, **49**(1), 574-589.
- 522 102. Peng, Y., Xu, Y., Cui, D., *CNS Neurol. Disord.*, 2014, **13**(5), 755-764.
- 523